

## NAVIGATION CONTROL AND STABILITY INVESTIGATION OF A HEXACOPTER EQUIPPED WITH AN AERIAL MANIPULATOR

Ibrahim N. Ibrahim, Kalashnikov Izhevsk STU, [ibrncfe@gmail.com](mailto:ibrncfe@gmail.com)

Božek Pavol, Slovak Univ. of Tech., Slovakia, [pavol.bozek@stuba.sk](mailto:pavol.bozek@stuba.sk)

Al Akkad M. Aiman, Kalashnikov Izhevsk STU, Russia, [aimanakkad@yandex.ru](mailto:aimanakkad@yandex.ru)

Almaghout Karam, Univ. of Tehran, [k.maghout@gmail.com](mailto:k.maghout@gmail.com)

### ABSTRACT

*In this paper, the dynamics model of a hexacopter equipped with a robotic arm has been formulated using Newton-Euler's method and its stability was investigated. For disturbances emulation, a simplified pendulum method was used. This Hexacopter configuration was not covered in scientific papers before. The resulting model is a nonlinear, coupled, and underactuated dynamics model, which includes aerodynamic effects and disturbances because of equipping the hexacopter with a robotic arm. The purpose of the presented paper is to offer a comprehensive study of determining the inertia moments of the hexacopter using a simplified pendulum method, taking into consideration the effect of mass distribution and center of gravity changes, which are a result of the continuous movement of the manipulator during the hexacopter motion in the air. The experimental tests were made using solid works application and were evaluated using LabVIEW in order to get a complete view of the disturbances, which were inserted into the dynamics model. The overall aircraft model was driven by four classical PID controllers for the vehicle's attitude and altitude of a desired trajectory in the space. These controllers were used to get a good understanding of how to evaluate and validate the model to make it an anti-disturbance model, in addition to their ease of design and fast response, but they require development in order to get optimal results. In future, a precise trajectory will be defined, and the controllers will be developed in order to get robust stability using nonlinear techniques and artificial intelligence.*

### KEY WORDS

UAV, Hexacopter Dynamics, Disturbances, Nonlinear Control, Coupled and Underactuated Models, Newton-Euler Method, Compound-Pendulum Method, Parallel Axis Theory.

### 1. INTRODUCTION

This work focuses on modeling and simulation of a hexacopter type unmanned aerial vehicle (UAV). Choosing a hexacopter is challenging in the field of control because it is a highly nonlinear, multivariable and underactuated system. It has stationary flight and high maneuverability [1]. An underactuated system is a mechanical system in which the dimension of the configuration space exceeds

that of the control input space, that is, with fewer control inputs than the degrees of freedom [2]. Modeling of such a system is not a trivial problem due to the coupled dynamics of the aerial vehicle [3]. The contribution of this paper lies in simplifying the dynamic modeling of the flying object equipped with a robotic arm. By deducing the equations of motion, with the inclusion of direct disturbances that represent the robotic arm movement, by the equations of force and moment, in comparison with other works of Lucia [3] and Hasan [4], which relied on a complex mechanism through the mathematical modeling of certain arms of fixed design, and adding it to the flying object equations. This is considered limited, complex, and does not cover the changes that may occur in the air, and weather conditions to which the aircraft is exposed in the air far from laboratory conditions. The adopted disturbances in this research are produced based on compound-pendulum method [5] [6] [7] [8] and studied to cover all the random changes that may face the aircraft, and which cannot be considered as constants. This method gives a complete and clear picture of the disturbances that are affecting the inertia moment, center of gravity and mass distribution in the coordinate frame of the aircraft during its movement in the air. The experimental tests of disturbances were taken using SolidWorks application and were checked by mathematical calculations. This method, which was not mentioned in literature before gives a complete handling of noise determination and formulates random disturbances' functions [9] that were inserted into the dynamics model of the hexacopter. Inertial moments amounts were studied according to the overall aircraft model [10] [11] [12] [13], in addition to applying the theory of parallel axis of Huygens-Steiner [14], which is concerned with studying the new inertia moment of the studied part relative to new axis of study parallel to the axis of the part to be studied. The contribution of this research lies in deducing a precise and detailed mathematical model of a hexacopter type aircraft in comparison with other researches like Alvarez-Munoz [15] that relied on assumptions and simplifications to make the modeling easier like mass distribution and other parameters in the body of the aircraft. The equations of motion of the whole system were designed using the Newton-Euler formulation for translational and rotational dynamics of a rigid body [16][17][18]. The disturbances are presented as an environment for outdoors simulation, which is omitted in most of the scientific literature [3][4][15].

## 2. THE HEXACOPTER REFERENCE FRAMES

The hexacopter structure and the engineering design are illustrated in figure 1 including the earth inertial frame (E-frame) and the body-fixed frame (B-frame). The motion is planned by using geographical maps, with North, East, and Down (NED) coordinates [3][18]. This earth fixed frame is seen as an inertial frame in which the absolute linear position  $(x, y, z)$  of the hexacopter is defined. The mobile frame  $(X_B, Y_B, Z_B)$  is the body fixed frame that is centered in the hexacopter center of gravity (CG), and oriented as shown in figure 1. The angular position of the body frame with respect to the inertial one is defined by Euler angles: roll  $\phi$ , pitch  $\theta$  and yaw  $\psi$ . These together form the vector:  $\sigma = [\phi \ \theta \ \psi]^T$  where  $\phi$  and  $\theta \in ]-\frac{\pi}{2}, \frac{\pi}{2}[$ ;  $\psi \in ]-\pi, \pi[$ . The inertial frame position of the vehicle is given by vector  $\xi = [x \ y \ z]^T$  [19][17][20]. The transformation from the body frame to the inertial frame is realized by using the well-known rotation matrix  $C_b^n$  defined in [19][20], which is orthogonal and  $C_b^n^T = C_b^{n-1} = C_n^b$ . In addition, the transformation matrix for angular velocities from the body frame to the inertial one is  $S$  as mentioned in [11]. where  $\dot{\sigma} = S \cdot \Omega$ ,  $\dot{\xi} = C_b^n \cdot V$ , the angular velocity  $\Omega$  is defined by the vector  $\Omega = [p \ q \ r]^T$ , and the linear velocity is defined by the vector  $V = [u \ v \ w]^T$  in the body frame. It is important to observe that  $S$  can be defined if and only if  $\theta \neq \frac{\pi}{2} + \pi k$ :  $k \in \mathbb{Z}$ . This is the main effect of Euler's formulation that leads to the gimbal lock, typical situation in which a degree of freedom is lost [22][23], which is not considered here.

## 3. THE HEXACOPTER DYNAMICS

The mathematical equations of the hexacopter dynamical behavior are derived by generalizing the quadcopter model presented in [21]. Newton-Euler equations that govern linear and angular motion are used, assuming that the hexacopter is a rigid body with a symmetrical structure. Therefore, the equations with respect to the body frame are:

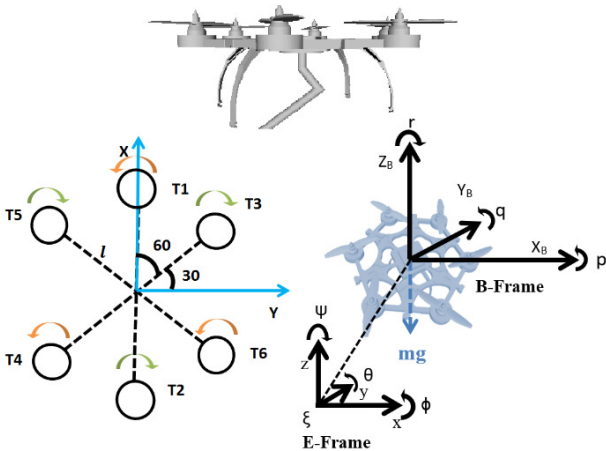


Figure 1. Hexacopter UAV structure and frames.

$$\begin{aligned} \dot{u} &= -\frac{k_t}{m}u + g \cdot \sin\theta - (qw - vr) + \frac{F_{d1}}{m} \\ \dot{v} &= -\frac{k_t}{m}v - g \cdot \sin\theta \cdot \cos\theta - (ru - pw) + \frac{F_{d2}}{m} \\ \dot{w} &= \sum_{i=1}^6 |T_i| - \frac{k_t}{m}w - g \cdot \cos\theta \cdot \cos\theta - (pv - qu) + \frac{F_{d3}}{m} \\ \dot{p} &= \frac{\sqrt{3}}{2l_x} (|T_3| - |T_4| + |T_6| - |T_5|) - \frac{k_r}{J_x} p - q r \frac{(J_z - J_y)}{J_x} + \frac{M_{d1}}{J_x} \\ \dot{q} &= \frac{1}{2l_y} (|T_3| - |T_4| + |T_5| - |T_6|) + \\ & 2(|T_1| - 2|T_2|) - \frac{k_r}{J_y} q - p r \frac{(J_x - J_z)}{J_y} + \frac{M_{d2}}{J_y} \\ \dot{r} &= \frac{\rho C_Q A R^3}{J_z} (\omega_1^2 + \omega_4^2 + \omega_6^2 - \omega_2^2 - \omega_3^2 - \omega_5^2) - \frac{k_r}{J_z} r - p q \frac{(J_y - J_x)}{J_z} + \frac{M_{d3}}{J_z} \end{aligned}$$

where  $m \in \mathbb{R}$  is the hexacopter total mass,  $g$  is the gravity constant,  $l$  is the distance from CG to the center motors,  $J \in \mathbb{R}^3$  is the diagonal inertia matrix,  $J_x, J_y$  and  $J_z$  are inertial moments of the rigid body along axes.  $F_{dist} = [F_{d1} \ F_{d2} \ F_{d3}]^T$ , and  $M_{dist} = [M_{d1} \ M_{d2} \ M_{d3}]^T$  are respectively the disturbance forces and moments along the axis.  $T_i$  And  $\omega_i$  (where  $i = 1 \dots 6$ ) are the thrust and angular moments of the motors as shown in figure 1,  $k_t$  and  $k_r$  are respectively the constants of aerodynamic force and moment,  $C_Q$  is the motor's torque coefficient,  $\rho$  is the air density,  $A$  is the propelling disc area, and  $R$  is the disc radius [3][16][17][20]. The propeller's thrust and torque, are [16]:  $T = \rho C_T A R^2 \omega^2$ , and  $Q = \rho C_Q A R^3 \omega^2$ , where  $C_T$  is the thrust coefficient [16]. The equations of motion that governs the hexacopter's translational and rotational motion with respect to the Earth frame are:  $\dot{\xi} = C_b^n \cdot V$ ,  $\dot{\sigma} = S \cdot \Omega$ . From the control problem, which govern the attitude and altitude in space, the artificial vector  $U = [u_p \ u_r \ u_y \ u_r]^T$  can be found. This simplifies the control of the system and instead of using real motors' velocities, vector  $\omega = [\omega_1 \ \omega_2 \ \omega_3 \ \omega_4 \ \omega_5 \ \omega_6]^T$  is used [17]. Then the equations that connect the artificial and real input vectors as follows:

$$\begin{cases} \omega_1 = u_T + u_p + u_y \\ \omega_2 = u_T - u_p - u_y \\ \omega_3 = u_T + 0.5 * u_p - 0.866 * u_r - u_y \\ \omega_4 = u_T - 0.5 * u_p + 0.866 * u_r + u_y \\ \omega_5 = u_T + 0.5 * u_p + 0.866 * u_r - u_y \\ \omega_6 = u_T - 0.5 * u_p - 0.866 * u_r + u_y \end{cases}$$

## 4. STUDYING THE DISTURBANCES OF THE ARM MOVEMENT IN SPACE

Figure 2 shows the complete hexacopter's mathematical model with added disturbances that represent an attached robotic arm with a payload. The disturbances affecting the aircraft's center of gravity change with time, due to the change in the robotic arm angles in all directions, making the motion equations variable with time, too. The arm movement with a payload is represented as a compound-pendulum, adopting the mathematical procedure in [5][6][7][8]. The disturbances parameters in the motion equations are based on the pendulum model. A rectangular aircraft shape was chosen as in figure 3. The pendulum motion takes place according to the angles of motion  $(\theta_1,$

$\theta_2, \theta_3$ ) as illustrated in figure 3, and these angles ranges are  $(0 < \theta_1 < 360, -5 < \theta_2 < -175, -155 < \theta_3 < 155)$ . Assuming, the weight of the payload is fixed, leads to changes in the aircraft's center of gravity, overall inertia moment, and in the thrust of aerial motors resulting from distance change between the aircraft's center of gravity and each engine. The general form of disturbances can be expressed as follows [9]:

$$F_{dist} = f_F(\theta_1, \theta_2, \theta_3), M_{dist} = f_M(\theta_1, \theta_2, \theta_3).$$

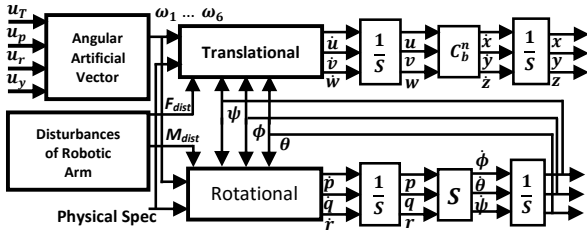


Figure 2. Block diagram of the hexacopter dynamics system.

assuming that the pendulum motion occurs when the aircraft hovering position is fixed, therefore the aerodynamic effects resulting from airflow through the pendulum become neglected. The change in the overall center of gravity and the inertia moment will be studied mathematically and compared with the simulation measurements. Assuming the initial values of the pendulum angles are:  $(\theta_1 = 0^\circ, \theta_2 = -5^\circ, \text{ and } \theta_3 = -155^\circ)$ , and according to the physical characteristics defined in figure 3, the pendulum's characteristics are in table 1, where the aircraft's overall center of gravity is defined by the  $X_B, Y_B, Z_B$  coordinates. In comparison with the aircraft's overall center of gravity, each part of the pendulum has a local coordinate system that coincides with the local center of gravity of that part as shown in figure 4.

Table 1. General Specifications of the overall aircraft model

$M_b =$	$M_J =$	$M_{I1} =$	$M_{I2} =$	$M_l =$
25.0Kg	0.253Kg	1.03Kg	0.78Kg	7.0Kg

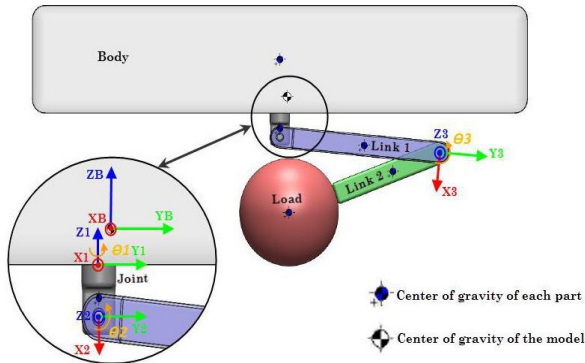


Figure 3. General model of the pendulum movement disturbances

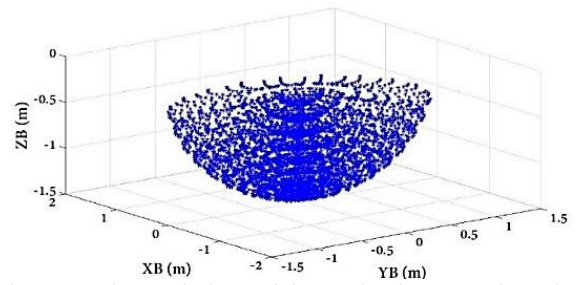


Figure 4. The workplace of the payload center of gravity.

#### 4.1 STUDYING THE CENTER OF GRAVITY CHANGE:

Studying the pendulum's motion workspace using computerized simulation, the payload's center of gravity draws a half sphere-like shape as in figure 4. Due to these changes, the aircraft's dynamics model center of gravity will change accordingly through the aircraft body axis  $X_B, Y_B, Z_B$ , as in figure 5. These changes are considered similar to half-sphere shape too. From the curves and table 2, the maximum value reached by the model's centers of gravity elements can be defined.

Table 2. Maximum values reached by the elements of the disturbances in the center of gravity.

	$X_B$	$Y_B$	$Z_B$
Max (m)	0.2602	0.005475	0.3093
Min (m)	-0.3173	-0.2359	-0.2683

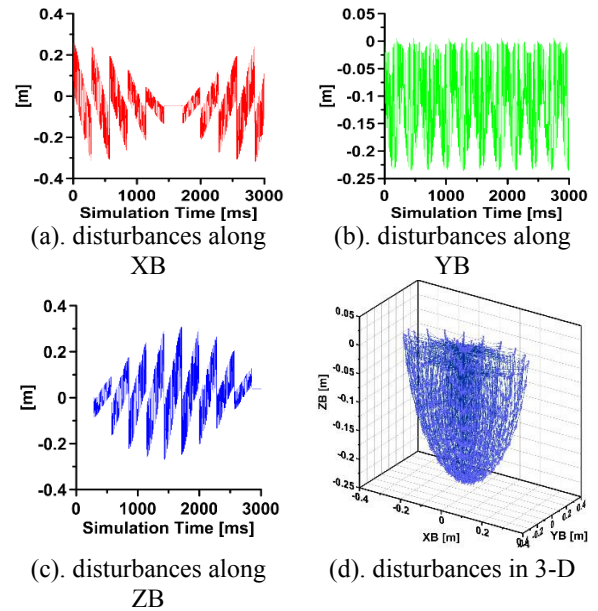


Figure 5. The disturbances in the center of gravity.

#### 4.2 STUDYING THE INERTIA MOMENT:

The inertia mass moment of complex shaped bodies is calculated using experimental methods. The mathematical study was simplified by dividing the overall aircraft model

into several parts that were studied separately. The goal is to determine the amount of inertia moment of the overall aircraft model according to the basic coordinate system XB, YB, ZB [10]:

$$J = J_{Body} + J_{Link1} + J_{Link2} + J_{Joint} + J_{Load}$$

where  $J$  is the inertia moment matrix of the overall aircraft dynamics model and  $J_{Body}$ ,  $J_{Joint}$ ,  $J_{Link1}$ ,  $J_{Link2}$ ,  $J_{Load}$  are the inertia moment matrices of the aircraft body, the joints, the 1<sup>st</sup> and 2<sup>nd</sup> links, and the load. The inertia for each part is studied using the theory of parallel axis of Huygens-Steiner [14], as in:  $J_0^* = J_0 + M \cdot d^2$ , where  $J_0$  is the new inertia moment of the studied part relative to new axes parallel to the output coordinates system by the angles  $\alpha$ ,  $\beta$ ,  $\gamma$ , as shown in figure 6. While  $J_{xx}$ ,  $J_{yy}$ ,  $J_{zz}$ ,  $J_{xy}$ ,  $J_{xz}$ ,  $J_{yz}$  are the studied part's local inertia moment matrix elements. The Curves in figures 7 to 12 illustrate the disturbances in the inertia moments of the aircraft's overall dynamics model relative to the pendulum's angles change range. From the curves and table 3, the maximum values of the inertia moments' matrix elements are defined. Table 4 shows the errors between the simulation results and the theoretical calculations of specific values of the pendulum's angles. These results are shown in figure 13 and emulated based on the change of the inertia moments and the center of gravity. The hexacopter parameters correlation was analyzed in figure 14. From figure 2 it is noticeable that this affects indirectly the translational and rotational aircraft motion. The curves in figure 14, show that controlling the pitch angle led to an indirect effect on the other angles and on the angle change rate, that means, the controllers should be faster than the rate of angle change in order to avoid vibrations. The oscillations, resulted from the attached robotic arm, and appeared in all attitude's variables and angles' rates, spread into other variables because of the coupling characteristic. The nonlinearity gives smooth shape to the curves, affecting the accuracy of control. The scenario here is a hovering flight at an altitude of 10 meters. A real dynamics model was developed addressing the nonlinear, time-variant and underactuated problems.

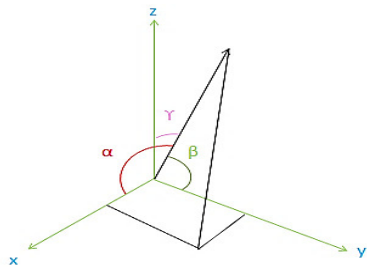


Figure 6. Angles of difference between the local axis of the studied body and the new axis.

## 5. PROPORTION, INTEGRAL, AND DERIVATIVE CONTROLLER DESIGN

Four linear and classical PID controllers were chosen to control attitude and altitude of the aircraft at desired trajectory in space, because of their ease of design and fast

response, and their parameters were tuned using Ziegler-Nichols algorithm [24] to get the best performance. The controllers' speed here is considered suitable as it enables tracking the vibrations and changes for avoiding the vibrations in the output. A mathematical model of PID is described as following equation [24]:

$$u(t) = k_c[e(t) + \frac{1}{T_i} \int e(t) \cdot dt + T_d \frac{d}{dt} e(t)]$$

Parameter  $k_c$  is the proportional gain,  $T_i$  is the integral time, and  $T_d$  is the derivative time. These parameters are defined, to get the best performance by decreasing vibrations, steady-state errors, and response time. Figure 15 shows the PID connection diagram, and the PID parameters are in table 5.

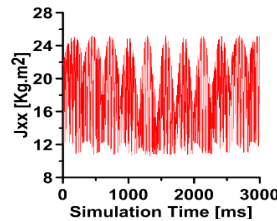


Figure 7.  $J_{xx}$  changes

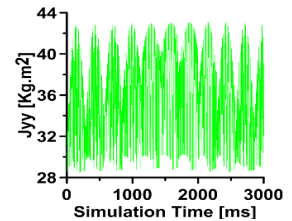


Figure 8.  $J_{yy}$  changes.

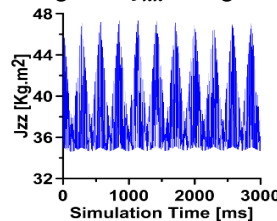


Figure 9.  $J_{zz}$  changes.

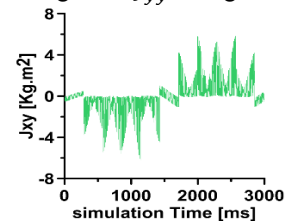


Figure 10.  $J_{xy}$  changes.

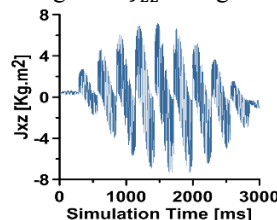


Figure 11.  $J_{xz}$  changes.

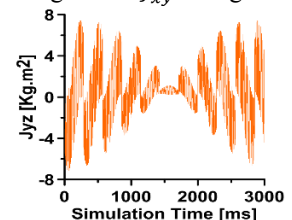


Figure 12.  $J_{yz}$  changes.

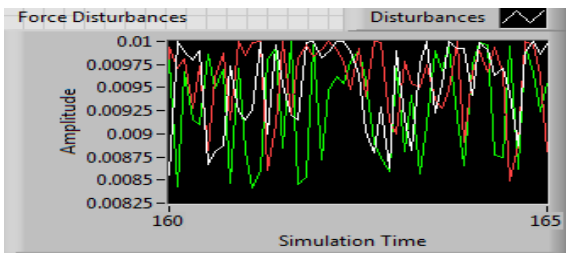
Table 3. Maximum values reached by the elements of the inertia moments matrix of the overall model

	$J_{xx}$	$J_{yy}$	$J_{zz}$	$J_{xy}$	$J_{xz}$	$J_{yz}$
Max	25.21	43.06	47.31	5.872	7.179	7.44
Min	10.67	28.42	34.65	-6.24	-7.45	-7.02

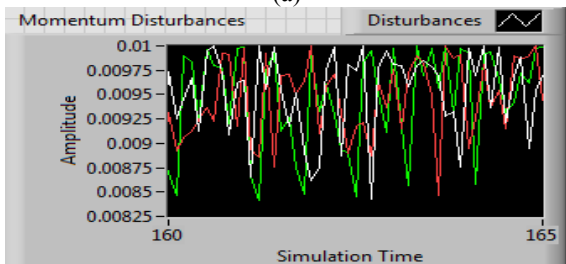
To control the hexacopter an application was conducted by LabVIEW using Runge-Kutta 2 method with a fixed step of 0.05 sec. The curves in figures 16 to 20 show the control signals and the responses with the existence of disturbances. These controllers avoid the occurrence of vibrations in the output. An analytic study of the controller's stability based on studying the unity response with several different levels of altitude and attitude is shown in table 6, Tuning has been achieved after many experimental trials. The scenario is a hovering flight at an altitude of multi-levels. The system's parameters used in the simulation, are listed in table 7.

Table 4. Errors between the calculated results based on SolidWorks program and the theoretical calculations

Moments of inertia kg. mm <sup>2</sup>	No.1	No.2	No.3
	$\theta_1^\circ=0$	$\theta_1^\circ=72$	$\theta_1^\circ=216$
	$\theta_2^\circ=-5$	$\theta_2^\circ=-158$	$\theta_2^\circ=-107$
	$\theta_3^\circ=-31$	$\theta_3^\circ=46.5$	$\theta_3^\circ=-62$
	Error %	Error %	Error %
$J_{xx}$	0.0000	0.2125	0.2131
$J_{yy}$	0.0026	0.1854	0.2225
$J_{zz}$	0.0017	0.2692	0.0955
$J_{yz}$	0.2319	1.6490	0.5049
$J_{xy}$	1.9312	2.0046	3.1939
$J_{xz}$	1.4129	0.3839	3.6553



(a)



(b)

Figure 13. Force and momentum disturbances resulted from the robotic arm.

## 6. CONCLUSIONS

A real and complex dynamic model was considered, which addresses the nonlinearity, time-variance, coupling, underactuation, and disturbances. This paper gives a complete discussion of the determination of the moments of inertia by simplified pendulum method, in addition to taking into consideration the effects of mass distributions and center of gravity change. These disturbances were inserted into the equations of motions, which also simulate a robotic arm motion while the aircraft model is flying in the sky. An application was conducted using SolidWorks and LabVIEW. The controllers' parameters were tuned using Ziegler-Nichols algorithm to get the best performance and avoid output vibrations. These controllers are suitable but not ideal and require improvement in order to get optimal results. Future work focuses on developing a precise trajectory control by using robust techniques including nonlinear techniques and artificial intelligence to stabilize the whole system and lead the hexacopter to the desired trajectory of Cartesian position, attitude, and airspeed.

**Acknowledgement:** The contribution is sponsored by VEGA MŠ SR No 1/0367/15 prepared project "Research and development of a new autonomous system for checking a trajectory of a robot".

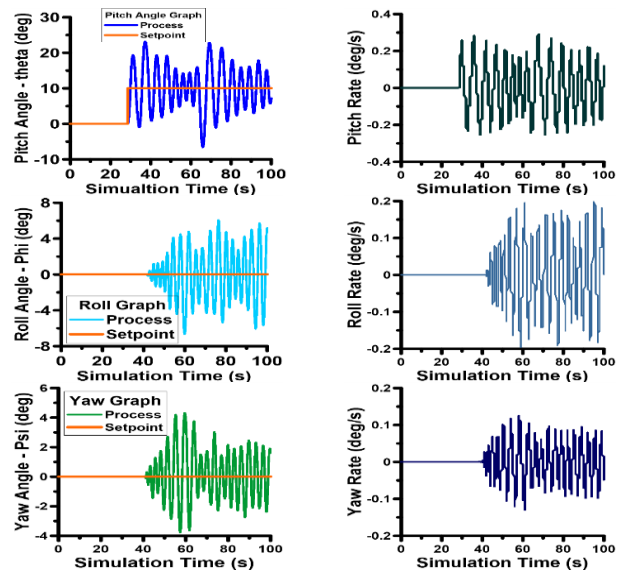


Figure 14. Stability study of the hexacopter variables due to change of input  $u_p$  with the existence of disturbances.

Table 5. PID controller parameters obtained by the Ziegler-Nichols Method.

Parameter	$u_T$	$u_p$	$u_r$	$u_y$
$k_c$	24.19	0.001	-0.00103	0.006
$T_i$	0.08299	6.1	6.3	20
$T_d$	0.01328	0.1	0.04073	0.4

Table 6. Stability Response of PID Controllers

PID Controller	Response Time (S)	Steady-State Error
Altitude	22.5	-0.0911 (m)
Pitch	8.15	0.01955 (deg)
Roll	5.72	0.0941 (deg)
Yaw	5.58	0.00173 (deg)

Table 7. Parameters used in the simulation

$m=4$ kg	$g=9.806$ m/s <sup>2</sup>	$l=0.5$ m
$J_x, J_y=3.8e^{-4}$ kg.m.s <sup>2</sup> /rad	$R=0.15$ m	$k_t=4.8e^{-3}$ kg.s/m
$J_z=7.1e^{-4}$ kg.m.s <sup>2</sup> /rad	$A=0.071$ m <sup>2</sup>	$k_r=6.4e^{-5}$ kg.m.s/rad
$C_T=0.01458$	$C_Q=1.037e^{-3}$	$\rho=1.293$ kg/m <sup>3</sup>

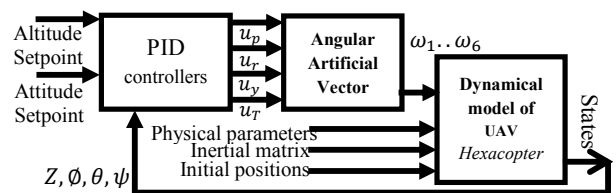


Figure 15. The block diagram of a PID controller connected to the hexacopter model

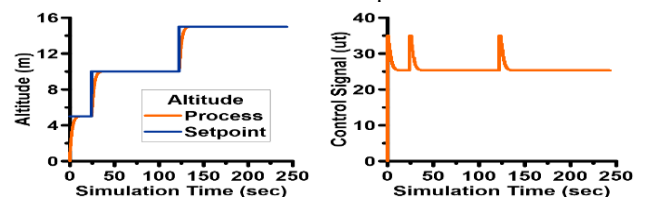


Figure 16. Stability response of altitude and control signal.

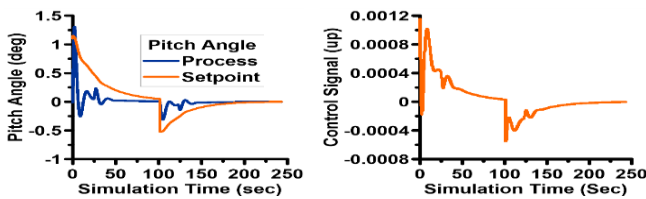


Figure 17. Stability response of pitch angle and control signal.

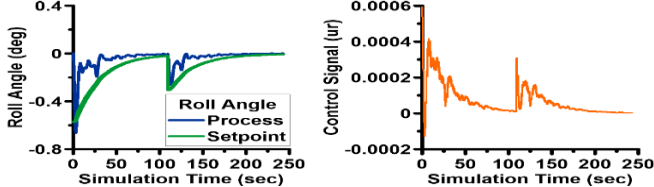


Figure 18. Stability response of roll angle and control signal.

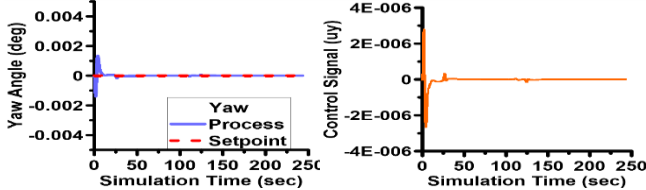


Figure 19. Stability response of Yaw angle and control signal.

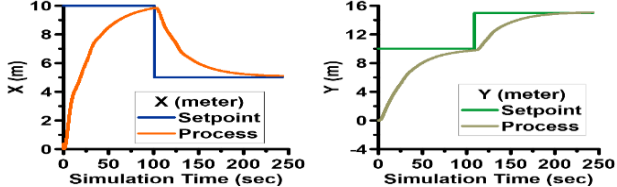


Figure 20. Stability response of X and Y coordinate systems.

## REFERENCES

- [1] M. D. Schmidt, *Simulation and Control of a Quadrotor Unmanned Aerial Vehicle*, Master's Theses, Lexington-USA, University of Kentucky University of Kentucky U Knowledge, 2011.
- [2] X. Xin, L. Yannian, *Control design and analysis for underactuated robotic systems*, Okayama University Japan, ISBN 978-1-4471-6251-3, 2014, Springer London.
- [3] S. D. Lucia, G. D. Tipaldi, W. Burgard, *Attitude Stabilization of an Aerial Manipulator using a Quaternion-based Back-stepping Approach*, IEEE-2015 European Conference, University of Freiburg Germany, 2-4 Sept.
- [4] Alvarez-Muñoz, J. U., et al, *Nonlinear control of a nano-hexacopter carrying a manipulator arm*, Intelligent Robots and Systems (IROS), 2015 IEEE/RSJ International Conference on. IEEE, 2015.
- [5] H. A. Soule, M. P. Miller, *The experimental determination of the moments of inertia of airplanes*, 1934.
- [6] W. Gracey, *The experimental determination of the moments of inertia of airplanes by a simplified compound-pendulum method.*, 1948.
- [7] J. Pobedonoszeff, *An Experimental Method of Determination of the Moments of Inertia of Aeroplanes*. Rep. No. 20l. Trans. CAHI, Moscow, 1935.
- [8] M. P. Miller, *An accurate method of measuring the moments of inertia of airplanes*, 1930.
- [9] J. Mathews, R. L. Walker, *Mathematical methods of physics*, vol. 501. New York: WA Benjamin, 1970.
- [10] F. S. Malvestuto, L. J. Gale, *Formulas for additional mass corrections to the moments of inertia of airplanes*, 1947.
- [11] M. V. Favorin, *Моменты инерции тел: Справочник*. Moscow, 1970.
- [12] G.B.Arften, H. J. Weber, and F. E. Harris, *Mathematical methods for physicists: a comprehensive guide*. Academic press, 2011.
- [13] M. M. Gernet, V. F. Ratobyl'skii, *Opredelenie momentov inertsii*. Publisher: Mashinostroenie, Place: Moscow, 1969, Pages: 247 pp.
- [14] T. R. Kane, D. A. Levinson, *Dynamics, theory and applications*. McGraw Hill, 1985.
- [15] J. U. Alvarez-Munoz, N. Marchand, J. F. Guerrero-Castellanos, A. E. Lopez-Luna, and S. Durand. *Improving Control of Quadrotors Carrying a Manipulator Arm*. CLCA 2014, Oct 2014, Mexico. 6p., 2014.
- [16] A. S. Sanca, T. L. Laura, J. F. Cerqueira, and P. J. Alsina, *Dynamic Modeling with Nonlinear Inputs and Backstepping Control for A Hexa-Rotor Micro-Aerial Vehicle*, Robotics Symposium and Intelligent Robotic Meeting (LARS), Latin American. IEEE ISBN 978-1-4244-8639-7, P36-42, 23-28 Oct. 2010.
- [17] M. Moussid, A. Sayouti, and H. Medromi, *Dynamic Modeling and Control of a HexaRotor using Linear and Nonlinear Methods.*, ISSN:2249-0868 Foundation of Computer Science FCS, Vol. 9, No.5, August 2015.
- [18] M. Moussid, A. Idalene, A. Sayouti, and H. Medromi, *Autonomous Hexa-rotor Aerial Dynamic Modeling and a Review of Control Algorithms*, International Research Journal of Engineering and Technology (IRJET) 2015, Vol. 02, Issue.05, August 2015: PP. 1197-1204.
- [19] D. Julián, M. Colorado, *Towards Miniature MAV Autonomous Flight: A Modeling & Control Approach*, Master thesis of Science in Robotics and Automation, Technical University of Madrid, April 2009.
- [20] O. Magnussen, K. E. Skjonhaug, *Modeling, Design and Experimental Study for a Quadcopter System Construction*, Master Thesis in Faculty of technology and science, University of Agder-Kristiansand S, Norway, 2011.
- [21] D. Sjolholm, M. Biel, *Automatic Control of a Quadrotor in the Smart Building*, KTH, School of Engineering Sciences (SCI), Master Thesis of Science in Engineering, KTH Royal Institute of Technology, Stockholm-Sweden, 2014.
- [22] V. Artale, C. L. R. Milazzo & A. Ricciardello, *Mathematical Modeling of Hexa-copter*, Applied Mathematical Sciences, Kore University of Enna, Italy, Vol. 7, 2013, no. 97, PP.4805 – 4811.
- [23] Chovancová, A., Fico, T., Chovanec, L. and Hubinsk, P., 2014. *Mathematical modelling and parameter identification of quadrotor (a survey)*. *Procedia Engineering*, 96, pp.172-181.
- [24] K. J. Astrom, R. M. Murray, *Feedback Systems*, Princeton University Press, ISBN-13: 978-0691135762, Vol.2, 11b, 2012.